The Photocatalytic, Thermal Degradation Kinetics and Lifetime Prediction of Some Commercial Reactive Dyes

Al-Maydama, Hussein M.*+; Al Kahali, Mohamed S.; Abduljabbar, Adlia A.; Aaad, Abdulbasset M.

Chemistry Department, Faculty of Sciences, Sana'a University, YEMAN

ABSTRACT: *The photocatalytic degradation of the commercial reactive Black5 (RB5), Blue19 (RB19), Green19 (RG19), Red120 (RR120), and Yellow81 (RY81) in aqueous solution and sunlight were examined in the presence of Fe_2O_3 and the mixture Fe_2O_3/H_2O_2 as catalysts. The results showed that the photocatalytic degradation followed first-order kinetics with faster degradation in case of the mixture Fe_2O_3/H_2O_2 than that in Fe_2O_3 catalyst. The photocatalytic degradation percentages with the exposure time intervals obtained for each dye were extrapolated to determine the time at the complete degradation (100% degradation). The thermal decomposition behavior of these dyes was investigated by using non-isothermal thermogravimetric analysis (TG, DTG, and DTA), at 10 °C/min heating rate and under nitrogen. The Coats-Redfern integral method was used for the five reactive dyes in order to evaluate the kinetic parameters for each step in the sequential decomposition TGA curves. The initial molecular structure destruction of these five reactive dyes occurred at their second steps. The kinetic parameters of this structural destruction step at multiple heating rates (10, 15, 20 and 30 °C/min) were only worked out for three selected dyes (RB5, RB19, and RR120) using the Flynn-Wall-Ozawa equation and compared with that of Kissinger's equation. Based on the data obtained by the Coats-Redfern method, the thermodynamic parameters (ΔG^*, ΔH^* and ΔS^*) for these second steps were determined. Finally, the kinetic data extracted from the TGA curves were also used as appropriate to predicate the lifetime of the five dyes at 25, 50, 100 and 200 °C.*

KEYWORDS: *Reactive dyes; Photocatalytic; Sunlight; TGA; Single heating rate; Multiple heating rates; Thermal stability; Degradation kinetics; Lifetime prediction.*

INTRODUCTION

Organic dyes are an abundant class of colored organic compounds that represent an increasing environmental danger. Some of these dyes are toxic and potentially carcinogenic [1]. Reactive dyes are extensively used in the textile industry because of their wide variety of color shades, simplicity of application, brilliant colors, and minimal energy consumption [2]. They mainly include azo, anthraquinone, triphendioxazine, phthalocyanine,

* *To whom correspondence should be addressed.*
+ *E-mail: hmaydama@yahoo.com*
1021-9986/2017/2/45-57 *13/$/6.30*

and formazan, which contain one or two functional groups capable of forming covalent bonds with the active sites in fibers. A carbon or phosphorous atom of the dye molecule will bond to hydroxyl groups in cellulose, amino, thiol, and hydroxyl groups in wool, or amino groups in polyamides [3, 4].

Heterogeneous photocatalysis through illumination of light to aqueous suspension of TiO_2 offers an attractive advanced oxidation process. This photocatalytic process is receiving great attention because of its mild operating conditions and it can be powered by sunlight. Another advanced oxidation process for the degradation of dyes is the UV photolysis in presence of H_2O_2. The photolysis of H_2O_2 is caused only by UV light and produce very reactive species of hydroxyl radical which can oxidize most of organic pollutants, therefore, higher efficiency of photocatalytic process is due to higher production of hydroxyl radicals [5]. Several studies have been reported the successful application of UV/H_2O_2 process for the treatment of dyes industrial wastewater [5–8].

The poor photocatalytic degradation using H_2O_2 was attributed to the slow photolysis of the H_2O_2 in sunlight because solar UV radiation contains very small part of total solar spectrum about 3.5-8%, therefore the low production of hydroxyl radicals from H_2O_2 was expected compared with that for artificial UV light [9].

The uses of Fe_2O_3 as a catalyst were a treated form of ferrioxalate, ferric nitrate, or ferrous sulphate, with H_2O_2 and light to produce Fe_2O_3 during the photolytic reaction [10-12]. As literature revealed no attempt of using directly Fe_2O_3/H_2O_2 and light in decomposing the dyes, this was an encouragement to us to use the mixture Fe_2O_3/H_2O_2 as a catalyst.

The application of some dyes for special uses and determining their thermal stabilities are very important [13]. The resistance to heat at elevated temperatures is one of the main properties required for the dyes used in high temperature processes such as dyeing, printing and photocopying and in high technology areas such as lasers and electro optical devices [14]. The decomposition of cyanine disperse dyes were reported thermally by *Emam et al.* [15, 16]. Some kinetic and thermodynamic parameters related to the thermal decomposition process of these dyes were calculated from their TG and DTA curves using single heating rate. In addition, azo dyes are of large interest from the point of view of possible applications. The thermal behaviors of these compounds using TG, DTG, and DTA curves were reported [17, 18]. Thermal studies of some aromatic azomonoethers were investigated and Caots-Redfern and Flynn-Wall-Ozawa methods were used to determine the kinetic parameters related to the decomposition of these azo dyes [19]. The processes of thermal decomposition of some new diazoaminoderivatives dyes were investigated by TG-FTIR [20-22].

In spite of the above mentioned studies reported on the thermal analysis of some dyes used in textile industry, and their calculated kinetic and thermodynamic parameters of the thermal decomposition process, yet there are no attempts have been made to study the thermal behavior of these commercial reactive dyes of interest.

This work compares the photocatalytic degradation of reactive dyes using Fe_2O_3/sunlight with that using Fe_2O_3/H_2O_2/sunlight. It also reports the thermal behavior, degradation kinetics, thermodynamic parameters and lifetime prediction at single heating rate (10 ˚C/min) and at the variety of heating rates (10, 15, 20 and 30 ˚C/min) for the decomposition of the commercial reactive dyes. The thermal data extracted from TGA curves are processed by the Caots-Redfern method [23] for single heating rate. However, for some selected dyes (RB5, RB19, and RR120) a Flynn-Wall-Ozawa [24, 25] and Kissinger [26] methods have been used at multi-heating rates of 10, 15, 20 and 30 ˚C/min.

EXPERIMENTAL SECTION

Materials

The commercially available reactive dyes of Black5 (RB5), Green19 (RG19), Red120 (RR120), and Yellow81 (RY81) from Rung International Company (India) and that of Blue19 (RB19) from Dankong Industry & Trade Group Co. Limited (China) were supplied by the Yemeni Company for Textile and Fibers.

The chemical formula, molecular structure, molecular mass and melting point of the five reactive dyes under investigation are illustrated in Scheme 1.

Photocatalytic degradation process

A certain concentrations of the reactive dyes (RB5, RB19, RG19, RR120, and RY81) aqueous solution were mixed with 1mg/mL Fe_2O_3 and 1mg/mL Fe_2O_3/ 0.1 M H_2O_2.

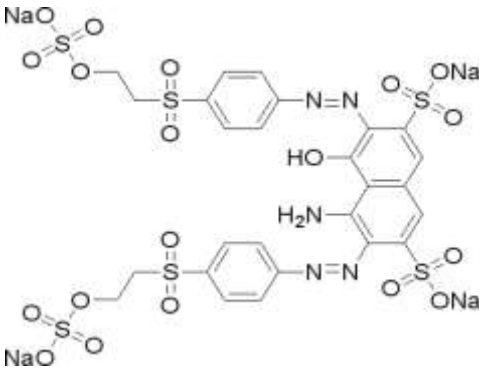

Reactive Black 5 (RB5)
M. wt: 991.82
Chemical Formula: $C_{26}H_{21}N_5Na_4O_{19}S_6$
Melting point: > 300 ˚C
λ_{max} : 603 nm

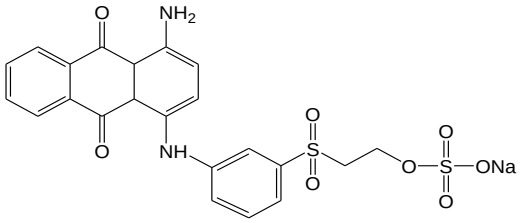

Reactive Blue19 (RB19)
M. wt: 626.54
Chemical Formula: $C_{22}H_{16}N_2Na_2O_{11}S_3$
Melting point: > 300 ˚C
λ_{max} : 596 nm

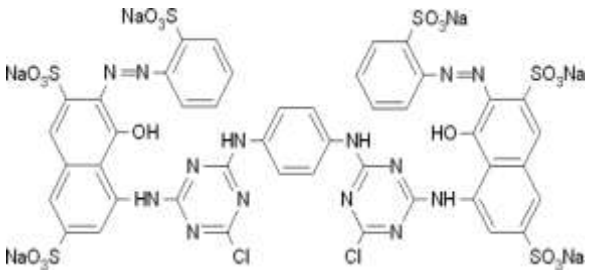

Reactive Red120 (RR120)
M. wt: 1469.98
Chemical Formula: $C_{44}H_{24}Cl_2N_{14}O_{20}S_6Na_6$
Melting point: > 300 ˚C
λ_{max} : 518 nm

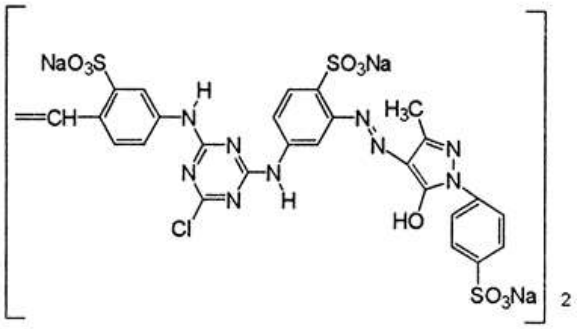

Reactive Yellow81 (RY81)
M. wt: 1632.17
Chemical Formula: $C_{52}H_{34}Cl_2N_{18}O_{20}S_6.6Na$
Melting point: > 300 ˚C
λ_{max} : 633 nm

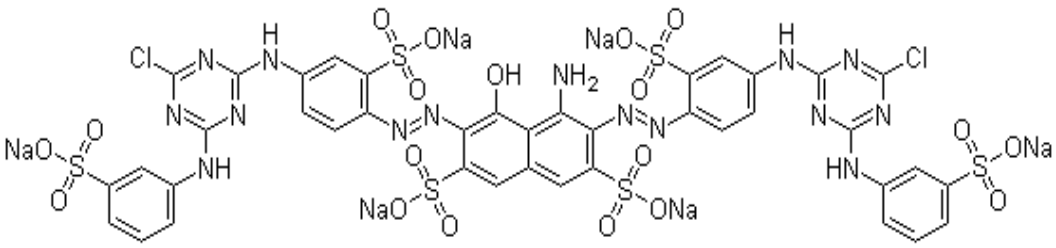

Reactive Green19 (RG19)
M. wt: 1418.95
Chemical Formula: $C_{40}H_{29}Cl_2N_{15}O_{19}S_6.6Na$
Melting point: > 300 ˚C
λ_{max} : 360 nm

Scheme 1: The reactive dyes under investigation (structure, molecular weight, and melting point).

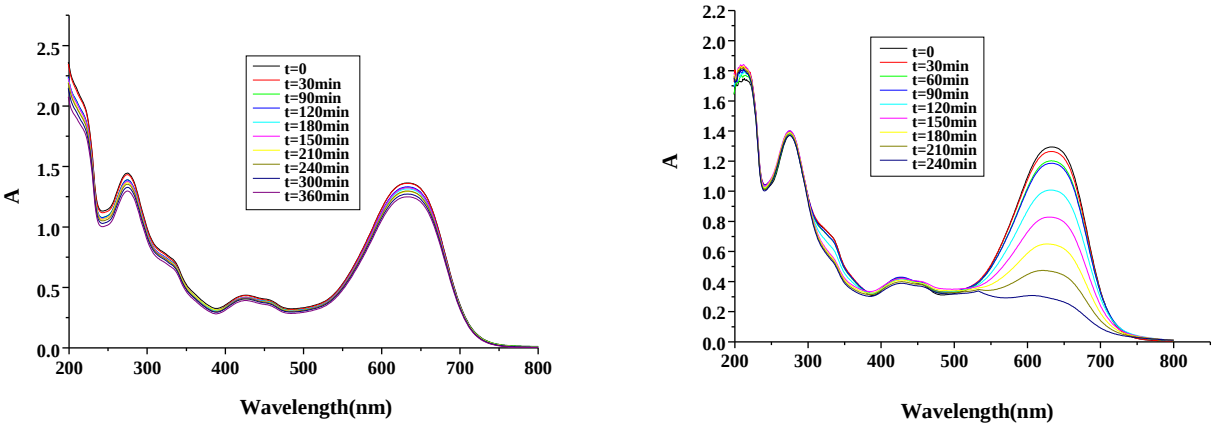

Fig. 1: Effect of sunlight on Reactive Green 19 (RG19) using: a) Fe_2O_3 b) Fe_2O_3/H_2O_2 as catalysts.

The samples were placed in open beakers and subjected to sunlight in sunny days of May (from 9:00 a.m. to 4:00 p.m.), with solar light intensity of about 2.96 $\times 10^{16}$ photons/sec. After irradiation at various time intervals, the samples were transferred into covered test tubes and then centrifuged for 30 min (4000 r.p.m).

UV- VIS Spectrophotometer (Specord200, Analytik Jena) was used to measure the absorbance of samples with time. The data of interest were calculated from the electronic spectra curves (λ_{max}) by applying the Beer-Lambert law.

Thermal analysis

The ThermoGravimetric Analysis (TGA) and Differential Thermal Analysis (DTA) of the reactive dyes (RB5, RB19, RG19, RR120, and RY81) were simultaneously measured by the Shimadzu DTG-60H thermal analyzers at a single (10 ˚C/min) and various heating rates (10, 15, 20 and 30 ˚C/min). Sample mass from 1.5 to 4 mg and Al_2O_3 as a reference were non-isothermally heated in nitrogen flow (20 mL/min) from 25 to 800 °CC.

Quantitative data were extracted from the relevant TGA curves in order to determine the kinetic parameters for all the five reactive dyes at a single heating rate (10 ˚C/min) by the *Coats-Redfern* method [23]. However, the kinetic parameters at various heating rates (10, 15, 20 and 30 °C/min) for only the molecular structure destruction process that occurred at the second steps of the three selected dyes (RB5, RB19 and RR120) were determined by using a *Flynn-Wall-Ozawa* [24, 25] and *Kissinger* [26] methods.

RESULTS AND DISCUSSION

Photocatalytic Degradation

The absorption spectra of degradation due to degrading benzene ring at UV region and of decolorization due to distraction of azo bonds (–N=N-) at visible region are evident in Fig. 1. The kinetic calculations of photocatalytic degradation are based on the decolorization at visible region. Changes in absorbance spectra with sunlight exposure time of the commercial reactive green 19 (RG19) dye in the presence of Fe_2O_3 and that of the Fe_2O_3/H_2O_2 mixture are shown in Fig. 1a and 1b. Significantly rapid degradation process is obvious in case of Fe_2O_3/H_2O_2 than that of Fe_2O_3. Similar results were obtained for RB5, RB19, RR120, and RY81 dyes. All samples showed a sequential profile decrease, and a decrease in the dyes concentrations is in succession with sunlight exposure time.

From the absorbance spectra, the concentration at a given exposure time is extracted. Therefore, the degradation percentage is calculated by using the following equation [27]:

$$\text{Degradation}\% = \frac{C_o - C_t}{C_o} \times 100$$

where C_o is the initial concentration, C_t is the concentration at a given exposure time.

The results of photocatalytic degradation of these reactive dyes in the presence of Fe_2O_3 and that of Fe_2O_3/H_2O_2 with given exposure times are collected in Table 1. The results in Table 1 regress satisfactorily (R^2= 99.9-96.1), and from which the exposure time for complete degradation of the dyes in Fe_2O_3 and in Fe_2O_3/H_2O_2 are extrapolated as given in Table 2.

Table 1: Degradation percentages of the reactive dyes and the given exposure times.

Time (min)	RB5		RB19		RG19		RR120		RY81	
	Fe_2O_3	Fe_2O_3/H_2O_2	Fe_2O_3	Fe_2O_3/H_2O_2	Fe_2O_3	Fe_2O_3/H_2O_2	Fe_2O_3	Fe_2O_3/H_2O_2	Fe_2O_3	Fe_2O_3/H_2O_2
15	0.059	1.6414	0.6906	0.0959	0.4657	2.747	1.186	0.0122	0.06	0.904
30	0.118	3.1829	1.3813	0.3918	0.9314	6.9094	2.077	0.025	0.98	1.408
45	0.398	4.1157	1.9528	1.6268	1.6135	14.6398	2.749	1.081	1.676	1.939
60	0.678	4.9485	2.5244	2.8686	2.2956	18.7702	3.025	2.137	2.055	2.67
75	0.73	6.2651	3.096	4.58837	2.4862	21.103	3.677	3.513	2.987	3.021
90	0.982	7.5817	3.6675	6.9749	2.9769	24.4348	4.383	4.89	3.418	3.372
105	1.214	8.5977	4.2391	8.9335	3.8463	30.922	4.922	6.2646	3.911	3.574
120	1.447	9.6137	4.8107	9.55215	4.4157	34.408	5.214	7.6403	4.033	3.776
135	1.588	10.892	5.3822	11.4465	4.8291	38.224	5.777	9.0161	4.513	4.128
150	1.71	12.7402	5.9538	13.8708	5.4425	43.839	5.941	10.392	4.91	4.479
165	1.754	13.8598	6.5254	14.7787	5.9665	47.983	6.418	11.768	5.251	5.291
180	2.099	15.3181	7.097	17.8166	6.8705	52.927	7.096	13.143	5.61	5.504
210	2.375	18.2092	8.2401	21.4577	7.7107	61.848	7.815	15.895	6.061	7.027
240	2.845	21.1003	9.3831	25.7732	8.3682	72.769	8.575	18.646	6.461	8.663
270	3.321	24.9914	10.526	28.6502	9.2536	79.793	9.571	21.398	7.463	9.907

Table 2: Half-life, rate constant and time of complete (100%) photocatalytic degradation of reactive dyes.

Reactive Dye	Fe_2O_3			Fe_2O_3/H_2O_2			Time reduction (%)
	k (min^{-1})	$t_{1/2}$ (h)	Time (h)	k (min^{-1})	$t_{1/2}$ (h)	Time (h)	
Black5	$1.17X10^{-4}$	98.7	132.5	$9.57X10^{-4}$	12.1	18.9	85.8
Blue19	$4.11X10^{-4}$	28.1	43.4	0.00109	10.6	15.4	64.4
Green19	$3.7X10^{-4}$	31.2	46.8	0.00466	2.5	5.5	88.2
Red120	$4.04X10^{-4}$	28.6	68.6	$7.84X10^{-4}$	14.7	19.5	71.7
Yellow81	$3.12X10^{-4}$	37.0	61.4	$3.55X10^{-4}$	32.5	50.7	17.4

Exposure times for complete degradation of these dyes in Fe_2O_3 and that in Fe_2O_3 / H_2O_2, together with the time reduced (i.e. time reductions %) due to the presence of H_2O_2 with Fe_2O_3 are compared in Table 2.

Exposure times of the dyes with Fe_2O_3 are significantly reduced by (88.2-17.4%), when compared with that in Fe_2O_3/H_2O_2. This can be seen in Table 2 as time reduction percentage. The catalyst Fe_2O_3 shows very slow degradation under sunlight [5]. Our attempt is to study the degradation of the dyes using hydrogen peroxide under sunlight, which did not work significantly, i. e. still slow but slightly better than Fe_2O_3. Therefore, an attempt to use Fe_2O_3 with the presence of H_2O_2 in order to compare the degradation with that of Fe_2O_3 is carried out. The rapid degradation of the dyes in Fe_2O_3/H_2O_2 can be attributed to the release of $OH^{\bullet}$ radicals due to the photolysis of H_2O_2 and the oxidation–reduction reaction of H_2O_2 with Fe^{3+} [10].

The kinetic curves of photocatalytic degradation of the reactive dyes were investigated by plotting the concentration (i.e. from Beer-Lambert law) against exposure time. At low initial concentration of most organic compounds, the kinetics of the photocatalytic degradation rate in liquid systems is described by pseudo first order kinetics [28]:

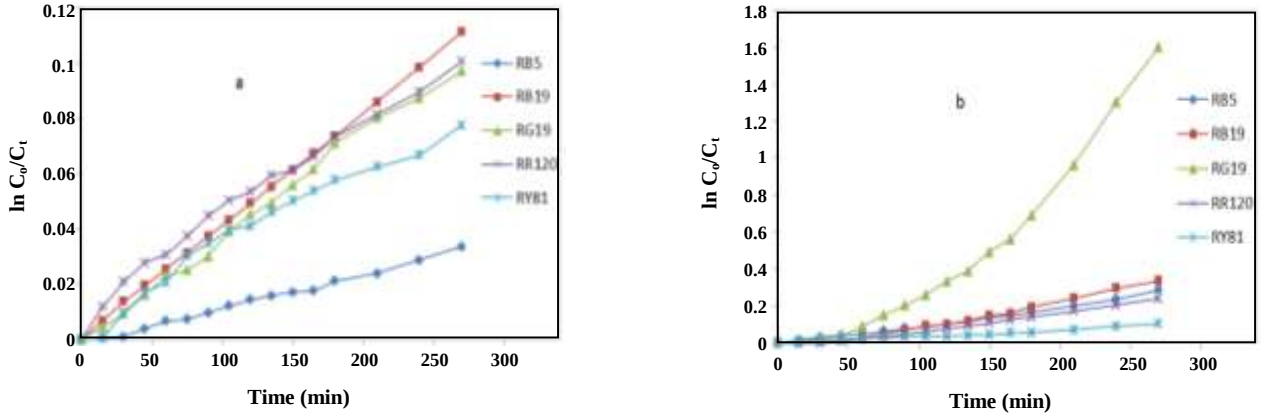

Fig. 2: Rate constants of decolorization of Reactive dyes using a) Fe_2O_3 b) Fe_2O_3/H_2O_2.

$$\ln\left(\frac{C_t}{C_o}\right) = -kt$$

where *k* is the rate constant, and *t* is the exposure time.

The plots of *ln* (C_t/C_o) versus *t* in Fig. 2 for each dye gave straight lines, from which the slope of linear variations equals to the apparent pseudo first-order rate constant *k*, (Table 2). All the experimental data obtained in this work were modeled to the single step first order reaction forming the products. Half-life of the dyes obtained from *k* is listed in Table 2. The values of half-lives of the dyes in Fe_2O_3 were vastly reduced in some cases than that in Fe_2O_3/H_2O_2 due to the production of $OH^{\bullet}$ radicals during the photocatalytic degradation reaction.

Thermal Degradation behavior

In thermogravimetric analysis, the conversion rate of reaction can be defined as the ratio of actual mass loss to the total mass loss corresponding to the degradation process.

$$\alpha = \frac{M_o - M}{M_o - M_f}$$

where: *M*, M_o, and M_f are the actual, initial, and final masses of the sample, respectively.

The characteristics of the thermal decomposition of the five reactive dyes recorded on TG–DTG–DTA curves under nitrogen atmosphere and their kinetics parameters at 10 ˚C/min heating rate are given in Table 3. Close examination of the TGA curves reveals that the investigated dyes decompose with a variety of numerous steps (three to four steps). The corresponding DTA data (Table 3) reveal that the decomposition processes of these dyes are thermally inconsistent with each other, i.e. some are exothermic and the others are endothermic. In general, the rapidity of these dyes' decomposition process can be described as a slow. In all reactive dyes, the mass losses (2.67%-8.31%) in the first steps were attributed to the elimination of one to five and half adsorbed water molecules (cal. 2.79-8.33%) endothermally.

The initial destruction of the dyes molecular structure occurs at the second steps (83.3 – 311.5˚C). Therefore, the dye RG19 exhibited the lowest decomposition temperature (83.3˚C), probably due to its highest structural steric hindrance, whereas the dye RY81 is of the highest one (311.5˚C) due to, maybe, the lowest steric. A slow and continuous bleeding of the molecular structure composition at several steps (i.e. two to three steps) with very high residue (46-69%) at the end is observed as a general feature for these dyes' decomposition process, as given in Table 3. As a result, these reactive dyes exhibit complicated thermograms. This is maybe for being hardly combustible material and having high molecular weight (626.54-1632.17 g/mol).

The initial decomposition temperature (T_i), after the release of the adsorbed water molecules, can be used as a measure of thermal stability [29, 30], i.e. the thermal stability increases as T_i increases. If the initial molecular structure destruction temperature (T_i) of the reactive dyes is taken as a measure of the thermal stability, the thermal stabilities of these reactive dyes follow the order: RY81 (311.5 ˚C) > RR120 (237 ˚C) > RB5 (213.4 ˚C) > RB19 (202.5 ˚C) > RG19 (83.3 ˚C). This indicates different thermal stabilities. RG19 is of the lowest stability (83.3˚C), whereas RY81 is of the highest one (311.5 ˚C).

Table 3: Thermal decomposition and kinetic parameters of the reactive dyes, by Coats-Redfern method at 10˚C/ min.

dye	Step	n	E_a kJ/.mol	TGA			DTA		Δm % found (cal.)	log Z S^{-1}	Reaction
				T_i ˚C	T_f ˚C	T_{max}˚C	T_{DTA}	Peak			
RB5	1	5	138.6	32.7	116.9	50.5	58.4	endo	8.31(8.33)	22.2	-5H_2O
	2	2.6	123.1	189	381.4	288.2	276.2	exo	13.58(13.58)	10.84	-14.81% of comp.
	3	1.5	181.6	381.4	466.5	436.2	456.7	endo	6.38 (6.38)	13.2	-6.96% of comp.
	4	0.9	147	466.5	648	578.7	570.4	exo	25.67(25.67)	8.4	-28% of comp.
	Total mass loss = 53.94% (found), 53.96% (cal.); Residue = 46.06% (found), 46.04% (cal.)										
RB19	1	2.4	82.2	24.1	118.6	46.2	-	-	2.67 (2.79)	11.8	-H_2O
	2	2.85	245.03	213	309.4	265.3	270.4	exo	4.15 (4.15)	23.6	-4.27% of comp.
	3	1.25	163.4	374.2	500.3	464	473.2	exo	18.46(18.46)	11.1	-19% of comp.
	4	2.4	370.8	500.3	620.7	545.9	552.9	exo	20.45(20.45)	23.3	-21.04% of comp.
	Total mass loss = 45.73% (found), 45.85% (cal.); Residue = 54.27% (found), 54.15% (cal.)										
RG19	1	1.7	110	27.8	83.3	59.1	-	-	4.10 (4.25)	17.7	-3.5H_2O
	2	1.8	69.1	83.3	183.2	98.2	-	-	3.3 (3.3)	8.8	-3.45% of comp.
	3	1.25	80.4	290.5	466.8	407	-	-	14.04(14.04)	5.6	-14.67% of comp
	4	1.3	91	466.8	725.3	631.9	651.3	endo	23.23(23.23)	5.5	-24.26% of comp.
							719.8	exo	-		Phase change
	Total mass loss = 44.67% (found), 44.82% (cal.); Residue = 55.33% (found), 55.18% (cal.)										
RR120	1	3	60.4	24.6	126.8	68	52.2	endo	6.29 (6.31)	8.9	-5.5H_2O
	2	1.55	55. 9	237	561	424.8	432.8	endo	24.35(24.35)	3.4	-26% of comp.
	3	0.8	97.6	561	801.7	728.3	569.4	endo	21.1 (21.1)	4.3	-22.51% of comp.
							740.4	endo	-		Phase change
	Total mass loss = 51.74% (found), 51.76% (cal.); Residue = 48.26% (found), 48.24% (cal.)										
RY81	1	1.8	44.7	27	137.4	48.8	103.3	endo	5.21 (5.23)	6.5	-5H_2O
	2	0.8	63.6	311.5	538.5	455.8	-	-	10.0 (10.0)	6.4	-10.55% of comp.
	3	1.6	176.3	538.5	706.7	657.1	621.2	endo	9.44 (9.44)	9.4	-9.96% of comp.
	4	1.8	364.9	706.7	801.3	725	691.4	endo	-	18.3	Phase change
							737.7	exo	6.31 (6.31)		-6.66% of comp.
	Total mass loss = 30.96% (found), 30.98% (cal.); Residue = 69.04% (found), 69.02% (cal.)										

Kinetic analysis

For the evaluation of the thermal degradation kinetics parameters of the five reactive dyes, a single heating rate method and two various heating rates methods are used in this study to calculate the activation energy (E_a) and pre-exponential factor (Z). The methods are:

Single heating rate: Caots-Redfern method

Coats-Redfern method [23], at a single heating rate (10 °C/min), is used to evaluate the activation energy (E_a) for each step in the sequential decomposition (Table 3). The equations used are:

$$\log\left[\frac{1-(1-\alpha)^{1-n}}{T^2(1-n)}\right]=\log\left[\frac{ZR}{qE_a}\left(1-\frac{2RT}{E_a}\right)\right]-\frac{E_a}{2.303RT} \quad \text{for } n\neq 1 \quad \rightarrow 1$$

$$\log\left[\frac{-\log(1-\alpha)}{T^2}\right]=\log\left[\frac{ZR}{qE_a}\left(1-\frac{2RT}{E_a}\right)\right]-\frac{E_a}{2.303RT} \quad \text{for } n=1 \quad \rightarrow 2$$

Where: α = fraction of weight loss, T = temperature (K), Z = pre-exponential factor, R = molar gas constant, q = heating rate and n = reaction order.

The reaction order value (n) determines the proper equation, and its correct value for a given thermal decomposition reaction gives a straight line. From equation 1 or 2, as appropriate, the activation energy of the decomposition process is calculated from the slope of the best straight lines ($r \approx 1$), whereas, the pre-exponential factor (*Z*) from the intercept for a given temperature, i.e. $T_{max.}$

Concerning the molecular weight and the second step where the destruction of dyes' structures commence, the RB19 with the lowest molecular weight (627 g/mol) and the lowest steric hindrance shows the highest activation energy (E_a = 252 kJ/mol). This is also observed in RB5 (E_a = 123 kJ/mol) of somewhat high molecular weight (992 g/mol) and high steric hindrance. However, those with the highest molecular weight, i.e. RG19 (1419 g/mol), RY81 (1632 g/mol) and RR120 (1470 g/mol) possess very low E_a (69, 64 and 56 kJ/mol, respectively). The lower E_a (69 kJ/mol) and of the lowest T_i (83°C) values of RG19 may be due to the highest steric hindrance in the molecular structure.

Various heating rates: Flynn-Wall-Ozawa (FWO) and Kissinger methods

To determine the activation energy from the slope of a straight line for the data recorded on the thermogravimetric curves at various heating rates, the following methods are used:

Flynn-Wall-Ozawa method [24, 25]:

$$\log\beta=\left[\log\left(\frac{ZE_a}{RF(\alpha)}\right)-2.315\right]-0.4567\left(\frac{E_a}{RT}\right) \quad \rightarrow 3$$

Kissinger method [26]

$$\log\frac{\beta}{T^2}=\log\frac{ZR}{E_a}-\frac{E_a}{2.303RT} \quad \rightarrow 4$$

Where β is the heating rate, T is the absolute temperature, R is the gas constant, α is the conversion of mass loss, E_a is the activation energy of the reaction and *Z* is the pre-exponential factor. Thus, at the same conversion (i.e. α = constant), the plot of log β against 1/T or log β/T^2 against 1/T, obtained from the TGA curves recorded for several constant-heating rates, should be a straight line whose slope could be used for the evaluation of the activation energy and the values of *Z* from the intercept.

Non-isothermal TGA of the samples was performed at heating rates of 10, 15, 20, 30 °C/min. The TG and DTG curves for the second steps of the RB5 pyrolysis at various heating rates are given in Fig. 3. It is obvious in Fig. 3 that the thermograms shift towards higher temperature with increasing β due to a shorter time required for the sample to reach a given temperature at a faster heating rate.

The effect of different temperature systems upon the thermal behavior of chemical compounds can provide kinetic parameters indicating change in the reaction course. The complexity of a stage can be expressed from the activation energy dependence on the conversion degree. For instance, if an activation energy (E_a) from isoconversional method does not depend on conversion degree (α), the investigated process is simple one and should be described by a unique kinetic triplet (E_a, *Z*, α). If activation energy changes with (α), the process is complex [19].

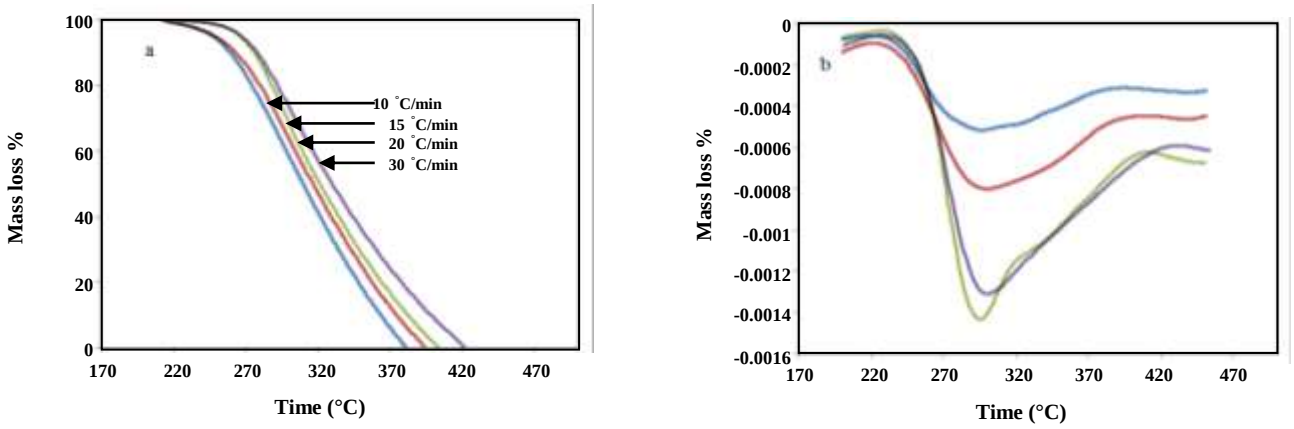

Fig. 3: (a) Mass loss% (TG), and (b) DTG curves for the second decomposition step of RB5 dye at heating rates 10, 15, 20, and 30 °C/min.

Vyazovkin and co-workers [31, 32] established an algorithm for identifying the type of complex processes. When E_a increases with conversion degree, the process involves parallel reactions. When E_a decreases and the shape of its evolution is concave, then the process has reversible stages. For decreasing convex shape, the process changes the limiting stage.

By applying equation (3) or (4) from 10 to 90% conversion for the initial structural degradation steps (i.e. second steps) of the RB5, RG19 and RR120 dyes are shown in Fig. 4. From the slope of the straight-line plot, the activation energy for any particular mass loss is evaluated. These conversional plots at different conversion values are almost parallel straight lines to each other (Fig. 4) and the accuracy in determining the activation energy was high (i.e. correlation coefficients are more than 0.99). This observation indicates that the decomposition process at the second steps of these three reactive dyes follows not complex mass loss process with several mechanisms, but a single-stage decomposition process [33]. The mean values of the activation energies and the pre-exponential factors of RB5, RB19, and RR120 second steps calculated by Kissinger, Ozawa-Flynn-Wall methods for 10-90% conversion and that values by the Coats-Redfern method (i.e. single heating rate) for all the five dyes along with their maximum rate temperatures (T_{max}) have been summarized and compared in Table 4. From Table 4, the highest standard deviation value of RR120 is self-evidence for a great activation energy variation with conversion. However, the lower one of RB5 and that of RB19 evidently reflects a slight variation with conversion. This clearly appears in the plots of activation energies against conversion degrees in Fig. 5.

Fig. 5 shows the *kinetic* results of the second decomposition steps of RB5, RB19 and RR120 obtained using FWO and Kissinger methods, as values of the activation energy for various conversion degrees from 10 – 90%. The activation energy (E_a) of RB5 slightly increases for the initial mass loss and after 10% conversion (20–50%) it remains constant, and then followed by slight decrease. For RB19, the activation energy slightly decreases for the initial mass loss and after 10% conversion it is approximately stable. However, RR120 shows increase of activation energy with conversion degree.

The activation energies of degradation for RB5 and RB19 remain relatively constant after 10% conversion, which reveal that there is one dominant kinetic process up to 10% conversion. In contrast, as the activation energy of RR120 increases with conversion complex process of parallel reactions takes place [33].

The activation energy of RB19 is lower than that of RB5 and of RR120 dyes as shown in Fig. 5. In general, the lower activation energy values of RB5 and RB19 dyes are attributed to increasing stability of the radicals formed during the pyrolysis process. On the other hand, the higher E_a values for RR120 are noticed in all conversions and it is consistent with its higher thermal stability [34]. It is also noticed that at 50% conversion, RR120 is of the highest E_a value (252.3 kJ mol^{-1}) than that of RB5 (157.47 kJ/mol) and of RB19 (111.8 kJ/mol).

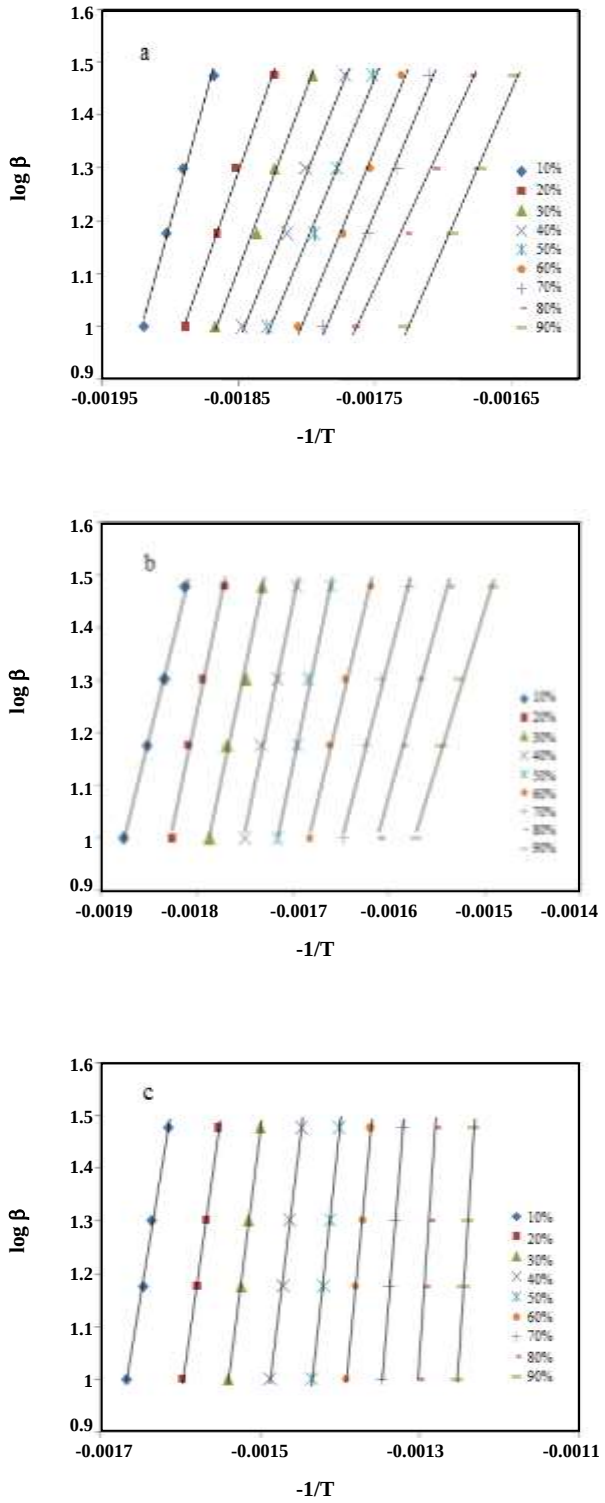

Fig. 4: Application of Flynn-Wall-Ozawa for the second decomposition step of RB19 (a), RB5 (b), and RR120 (c) at heating rates 10, 15, 20, and 30 ˚C/ min, from 10-90% conversion.

The results obtained by FWO and *Kissinger* methods are comparable. The differences in the values of the activation energy obtained using these two isoconversional integral methods may be attributed to the different approximations of the temperature integral they used [19].

The second decomposition steps of the dyes are of concern for being the initial molecular structure degradation step after the dehydration of the absorbed water. Based on the activation energy values from the slope of the Coats-Redfern plot and the corresponding pre-exponential factors and T_{nax} (Table 4), the thermodynamic parameters; enthalpy (ΔH^*), entropy (ΔS^*), and Gibbs energy (ΔG^*) of activation were calculated using the following standard equations:

$$\Delta S^* = R \ln \frac{Zh}{kT_{max}}$$

$$\Delta H^* = E_a - RT_{max}$$

$$\Delta G^* = \Delta H^* - T_{max}\Delta S^*$$

Table 4 gives the computed thermodynamic parameters for the five dyes under study. The positive values of ΔG^* and ΔH^* for the transition-state reaction imply a very small equilibrium constant and the reactants are stable with respect to the formation of the activated complex.

Except for the RB19 dye of the positive ΔS^*, the commonly negative values of the activation entropy changes for the structural degradation steps implies an increase in molecular order of the activated complex due to the conversion of transitional and rotational degrees of freedom of the reactant to vibrational degrees of freedom of the transition-state species [35].

Determination of lifetime prediction (t_f)

From the TGA recorded for these commercial dyes, the lifetime was estimated at various temperatures. The lifetime estimate of any target molecule is the time when the decompositon reaches 5% [36], hence for $n \neq 1$ it can be estimated by:

$$t_f = \frac{(1-0.95^{1-n})}{Z(1-n)} \exp \frac{E_a}{RT} \quad (5)$$

Based on the kinetic data obtained (Table 4) and equation (5), the estimated lifetime at various temperatures for these commercial dyes decomposition

Table 4: Kinetic and thermodynamic parameters of the second decomposition steps of the dyes.

Compound	Method	E_a kJ/mol	Log Z Sec	T_{max} K	ΔG^* kJ/mol	ΔH^* kJ/mol	ΔS^* J/K mol
RB5	Kissinger	239.6 ± 18.7	12 ± 2.4				
	FWO	239 ± 18.9	12.3 ± 2.3				
	Coats-Redfern	123.1	10.8	561.2	139.4	118.4	- 37.2
RB19	Kissinger	117.5 ± 21.8	10.9 ± 2.6				
	FWO	120.6 ± 20.4	11.3 ± 2.4				
	Coats-Redfern	245	23.6	538.3	131.7	240.6	202.2
RR120	Kissinger	278.3 ± 93.9	20.3 ± 5.1				
	FWO	275.8 ± 90	20.1 ± 4.9				
	Coats-Redfern	55.9	3.4	697.8	180.9	50.1	- 187.5
RG19	Coats-Redfern	69.1	8.8	387.7	96.2	65.9	- 78
RY81	Coats-Redfern	63.6	6.4	728.8	152.7	57.5	- 130.6

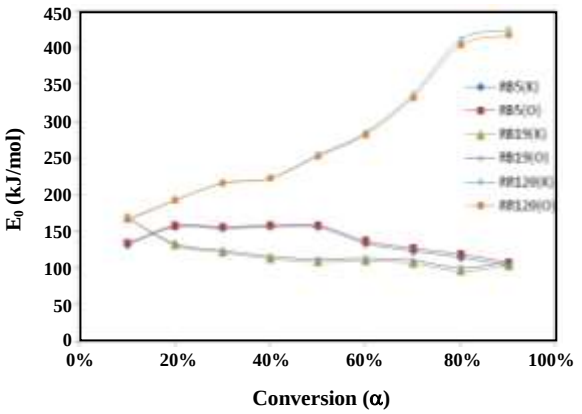

Fig. 5: Activation energies versus conversion degree for the second step of the reactive dyes (RB5, RB19, and RR120) degradation using Ozawa-Flynn-Wall (O) and Kissinger (K) methods.

are given in Table 5. It is apparent that the estimated lifetime values for the decomposition of RB5, RB19, RG19, RR120 and RY81 consistently vary with the temperatures at 25, 50, 100 and 200˚C.

On the other hand, since the time for 5% conversion of a target molecule at 25˚C is generally used to estimate a shelf life ($t_{5\%,\ 25°C}$) [37], RB19 exhibits the highest shelf life (3.73×10^{18} s), but RG19 is of the lowest one (106.15 s), as indicated in Table 5.

CONCLUSIONS

The photocatalytic degradation of the five dyes (RB5, RB19, RG19, RR120 and RY81) carried out in Fe_2O_3/sunlight and in Fe_2O_3/H_2O_2/sunlight obey first order kinetics. The photodegradation of these dyes are significantly rapid in Fe_2O_3/H_2O_2/sunlight than that in Fe_2O_3/sunlight and that in H_2O_2/sunlight.

The thermal analysis of these dyes was performed in nitrogen flow. The dehydration of the absorbed water molecules took place at the temperature range of 24-127 °C was followed by the molecular structure destruction steps at the range of 83 – 311 °C. The TGA curves of the dyes exhibited various decomposition steps; three to four decomposition steps. The kinetic parameters of these five dyes were evaluated using the Coats-Redfern equation at a single heating rate of 10 °C/min for each step in the decomposition sequence. The thermal stability on the bases of initial temperature was assigned.

For the second steps where the structural destruction occurred, the kinetic of RB5, RB19 and RR120 at various heating rates were determined using FWO and Kissinger methods. RB5 and RB19 showed lower activation energies with one dominant kinetic process up to 10% conversion, while RR120 experienced a complex process with higher activation energy. The thermodynamic parameters for the structural degradation steps were computed. The finding showed that the values of ΔG^*, ΔH^* *and* ΔS^* of these dyes were incomparable with each other. It is apparent that the values of lifetime of these dyes decrease dramaticaly as the temperatures increase. RB19 is of the highest shelf life (3.73×10^{18} s) and RG19 is of the lowest one (106.15 s).

Table 5: Estimated values of lifetime of the reactive dyes based on weight loss (α = 5%) at various temperatures.

dye	t_f (sec) at 5% conversion			
	25 ˚C	50 ˚C	100 ˚C	200 ˚C
RB5	3.20×10^{9}	6.84×10^{7}	1.47×10^{5}	33.28
RB19	3.73×10^{18}	1.43×10^{15}	4.97×10^{9}	1.74×10^{2}
RG19	106.15	12.27	0.390	0.004
RR120	1.30×10^{5}	2.27×10^{4}	1.39×10^{3}	30.86
RY81	2.86×10^{3}	3.92×10^{2}	16.38	0.214

Received : Apr. 4, 2016 ; Accepted : Nov. 1, 2016

REFERENCES

[1] Cisneros R.L., Espinoza A.G., Litter M.I., Photo Degradation of an Azo Dye of the Textile Industry, *Chemosphere*, **48**: 393-399 (2002).

[2] Lee Y.H., Pavlostathis S.G., Decolorization and Toxicity of Reactive Anthraquinone Textile Dyes under Methanogenic Conditions, *Water Res*., **38** (7): 1838-1852 (2004).

[3] Zollinger H., "Color Chemistry: Syntheses, Properties and Applications of Organic Dyes and Pigments", VCH Publishers, Weinheim, German (1991).

[4] Lewis D.M., Coloration for the Next Century, *Review of Progress in Coloration and Related Topics*, **29**: 23-28 (1999).

[5] Muruganadham M., Sobana N., Swaminthan M., Solar Assisted Photocatalytic and Photochemical Degradation of Reactive Black 5, *J. Hazardous Materials*, B**137**: 1371-1376 (2006).

[6] Marechal A.M.L., Slokar Y.M., Taufer T., Decoloration of Chlorotriazine Reactive Azo Dyes with H_2O_2/UV, *Dyes Pigments*, **33**: 281–298 (1997).

[7] Georgiou D., Melidis P., Aivasidis A., Gimouhopoulos K., Degradation of Azo-Reactive Dyes by Ultraviolet Radiation in the Presence of Hydrogen Peroxide, *Dyes Pigments*, **52**: 69–78 (2002).

[8] Neamtu M., Siminiceanu I., Yediler A, Kettrup A., Kinetics of Decolorization and Mineralization of Reactive Azo Dyes in Aqueous Solution by the UV/H_2O_2 Oxidation, *Dyes Pigments*, **53**: 93–99 (2002).

[9] Cho II-H, Kim L-H, Zoh K-D, Park J-H, Kim H-Y., Solar Photocatalytic Degradation of Groundwater Contaminated with Petroleum Hydrocarbons, *Environmental Progress*, **25** (2): 99-109 (2006).

[10] Jahagirdar A.A., Zulfiqar Ahmed M.N., Donappa N., Nagabhushana H., Nagabhushana B.M., Photocatalytic Degradation of Rhodamine B Using Nanocrystalline α-Fe_2O_3, *J. Mater. Environ. Sci.* **5** (5): 1426-1433 (2014).

[11] Cano-Guzmán C.F.,. Pérez-Orozco J.P, Hernández-Pérez I., L. González-Reyes I., Garibay-Febles V., Suárez-Parra R., Kinetic Study for Reactive Red 84 Photo Degradation Using Iron (III) Oxide Nanoparticles in Annular Reactor, *Textile Sci Eng*,**4** (2): 155 (2014).

[12 Neamtu M., Yediler A., Siminiceanu I., Kettrup A., Oxidation of Commercial Reactive Azo Dye Aqueous Solutions by the Photo-Fenton and Fenton-Like Processes, *J. Photochem. Photobiol. A: Chemistry*, **161**: 87-93 (2003).

[13] Masaund, M., Khalil, E., El-Sayed El-Shereafy, E., El-Enein S., Thermal and Electrical Behaviour of Nickel(II) and Copper(II) Complexes of 4-Acetylamino-2-Hydroxy-5-Methylazobenzene", *J. Thermal Anal.*, **36**: 1033-1038 (1990).

[14] Egli R., Color Chemistry: The Design and Synthesis of Organic Dyes and Pigments, Edited by. A. Peters, H. Freeman, Elsevier Applied science, London (1991).

[15] Emam M., Kenawy I., Hafez M., Study of the Thermal Decomposition of Some New Cyanine Dispersed Dyes, *J. Therm. Anal. Cal.*, **63**: 75-83 (2001).

[16] Emam M., Thermal Stability of Some Textile Dyes, *J. Therm. Anal. Cal.*, **66**: 583-591 (2001).

[17] Kocaokutgen H.H., Heren Z., Thermal Behaviour of Some Azo Dyes Containing Sterically Hindered and Water-Soluble Groups, *Turk J. Chem.*, **22**: 403 (1998).

[18] Kocaokutgen H., Gümrükçüoğlu I.E., Thermal Characterization of Some Azo Dyes Containing Intramolecular Hydrogen Bonds and Non-Bonds, *J. Therm. Anal. Cal.*, **71**: 675-679 (2003).

[19] Rotaru A., Moanț,ă A., Popa G., Rotaru P., Segal E., Thermal Decomposition Kinetics of Some Aromatic Aomonoethers: Part IV. Non-Isothermal Kinetics of 2-allyl-4-((4-(4-methylbenzyloxy) phenyl) diazenyl) Phenol in Air Flow, *J. Therm. Anal. Calorim.*, **97**: 485–491 (2009).

[20] Mocanu A., Odochian L., Apostolescu N., Moldoveanu C., TG-FTIR Study on Thermal Degradation in Air of Some New Diazoaminoderivatives, *J. Therm. Anal. Calorim.*, **100**: 615-622 (2010).

[21] Mocanu A., Odochian L., Moldoveanu C., Carja G., TG-FTIR Study on Thermal Degradation in Air of Some New Diazoaminoderivatives (II), *Thermochimica Acta*, **509**: 33-39 (2010).

[22] Mocanu A., Odochian L., Apostolescu N., Moldoveanu C., Comparative Study on Thermal Degradation of Some New Diazoaminoderivatives Under Air and Nitrogen Atmospheres, *J. Therm. Anal. Calorim.*, **103**: 283-291 (2011).

[23] Coats A.W., Redfern J.P., Kinetic Parameters from Thermogravimetric Data, *Nature*, **201**: 68 (1964).

[24] Ozawa T., A New Method of Analysing Thermogravimetric Data", *Bull. Chem. Soc. Jpn.*, **38**: 1881 (1965).

[25] Flynn J.H., Wall L.A., A Quick Direct Method for Determination of Activation Energy from Thermogravimetric Data, *J Polym Sci, B***4**: 323–8 (1966).

[26] Kissinger H.E., Reaction Kinetics in Deferential Thermal Analysis, *Anal Chem.*, **29**: 1702-6 (1957).

[27] Enes S., Optimization and Modeling of Decolorization and COD Reduction of Reactive Dye Solutions by Ultrasound-Assisted Adsorption, *Chem. Eng. J.*, 119: 175–181 (2006).

[28] Houas A.H., Lachhab M., Ksibi E., Elaloui C., Guillard C., Herrmann J.M., Photocatalytic Degradation Pathway of Methylene Blue in Water, *Appl. Catal. B: Environ.*, 31, 145-157 (2001).

[29] Al-Maydama H.M., El-Shekeil A.G., Al-Karbouly A., Al-Ikrimawy W., Thermal Degradation Behavior of Some Poly [4-amino-2,6-pyrimidinothiocarbamate] Metal Complexes, the *Arabian journal for science and engineering*, **34**(1): 67-75 (2009).

[30] Odochian L., Moldoveanu C., Carja G., Contributions to the Thermal Degradation Mechanism Under Air Atmosphere of PTFE by TG–FTIR Analysis: Influence of the Additive Nature, *Thermochimica Acta*, **558**: 22– 28 (2013).

[31] Vyazovkin, S., Lesnikovich, A. I., An Approach to the Solution of the Inverse Kinetic Problem in the Case of Complex Processes. Part 1: Methods Employing a Series of Thermoanalytical Curves, *Thermochim Acta*, **165**: 273–80 (1990).

[32] Vyazovkin S., Sbirrazzuoli N., Isoconversional Kinetic Analysis of Thermally Stimulated Processes in Polymers, *Macromol Rapid Commun.*, **27**: 1515–32 (2006).

[33] Wang H., Tao X., Newton E., Thermal Degradation Kinetics and Lifetime Prediction of a Luminescent Conducting Polymer, *Polym. Int.*, **53**: 20–26 (2004).

[34] Liu C., Yu J., Sun X., Zhang J., He J., Thermal Degradation Studies of Cyclic Olefin Copolymers, *Polym Degrad Stab.*, **81**: 197-205 (2003).

[35] Al-Maydama H.M., Comments on the Effect of UV Radiation on the Thermal Parameters of Collagen Degradation, *Polym Degrad Stab.*, **84**: 363-365 (2004).

[36] Xin-Gui Li, Huang M-R., Thermal Decomposition Kinetics of Thermotropic Poly(oxybenzoate-co-oxynaphthoate), *Polymer Degradation Stability*, **64**: 81-90 (1999).

[37] Prime R.B., Bair H. E., Vyazovkin S., Gallagher P.K., Riga A., Thermogravimetric Analysis (TGA). In Thermal Analysis of Polymers: Fundamentals and Applications, eds. J. D. Menczel and R. B. Prime. Hoboken, NY: Willey, 241–317 (2009).